Talanta 78 (2009) 1148–1154

Contents lists available at ScienceDirect

Talanta

journal homepage: www.elsevier.com/locate/talanta

An electrochemical biosensor for α-fetoprotein based on carbon paste electrode constructed of room temperature ionic liquid and gold nanoparticles

Caifeng Ding[a,b], Fei Zhao[b], Rui Ren[b], Jin-Ming Lin[a,*]

[a] The Key Laboratory of Bioorganic Phosphorus Chemistry & Chemical Biology, Department of Chemistry, Tsinghua University, Beijing 100084, PR China
[b] Key Laboratory of Eco-chemical Engineering, Ministry of Education; College of Chemistry and Molecular Engineering, Qingdao University of Science and Technology, Qingdao 266042, PR China

ARTICLE INFO

Article history:
Received 10 October 2008
Received in revised form 15 January 2009
Accepted 18 January 2009
Available online 24 January 2009

Keywords:
Electrochemical immunoassay
α-Fetoprotein (AFP)
Carbon paste electrode (CPE)
Gold nanoparticle
Room temperature ionic liquid (RTIL)
O-Aminophenol (OAP)

ABSTRACT

A novel and effective electrochemical immunosensor for the rapid determination of α-fetoprotein (AFP) based on carbon paste electrode (CPE) consisting of room temperature ionic liquid (RTIL) *N*-butylpyridinium hexafluorophosphate ($BPPF_6$) and graphite. The surface of the CPE was modified with gold nanoparticles for the immobilization of the α-fetoprotein antibody (anti-AFP). By sandwiching the antigen between anti-AFP on the CPE modified with gold nanoparticles and the secondary antibody, polyclonal anti-human-AFP labeled with horseradish peroxidase (HRP-labeled anti-AFP), the immunoassay was established. The concentration of AFP was determined based on differential pulse voltammetry (DPV) signal, which was generated in the reaction between *O*-aminophenol (OAP) and H_2O_2 catalyzed by HRP labeled on the sandwich immunosensor. AFP concentration could be measured in a linear range of 0.50–80.00 ng mL^{-1} with a detection limit of 0.25 ng mL^{-1}. The immunosensor exhibited high sensitivity and good stability, and would be valuable for clinical assay of AFP.

1. Introduction

Due to the highly sensitive and selective nature of the recognition between antigens and antibodies (Ab), immunoassays are very useful in many fields such as medical detection, processing quality control and environmental monitoring [1]. Conventional methods used in immunoassays, including enzyme-linked immunosorbent assay (ELISA), immunoradiometric assay (IRMA) and single radial immunodiffusion, usually have various limitations such as relying on the label of either antigen or antibody, radiation hazards, long analysis time, expensive instruments and skillful operators [2]. New techniques, such as electrochemistry [3], chemiluminescence [4], piezoelectricity [5] and surface plasmon resonance [6], have attracted extensive interests in immunoassays due to their simple and specific characteristics. Among these techniques, electrochemical immunoassay has received much attention for its high sensitivity and low cost. In electrochemical immunoassays, the target specific ligands must be effectively immobilized on the electrode surface and the analytes must be able to access their immobilized recognition couple under satisfactory frequency without severe steric hindrance and nonspecific binding [7]. Thus, the design and implementation of a unique sensing surface for facile ligand functionalization and biospecific interaction are crucial.

Carbon paste electrode (CPE), which was made up of carbon particles and organic liquid, has been widely applied in the electroanalytical community due to its low cost, ease of fabrication, high sensitivity for detection and renewable surface [8–13]. Generally, the organic liquid, as a binder component in the pastes, is a non-conductive mineral oil, which to some extent weakens the electrochemical response of CPE, thus is especially disadvantageous for the detection. Room temperature ionic liquids (RTILs), possessing unique properties such as negligible vapor pressure, wide potential windows, high thermal stability and high viscosity and good conductivity and solubility, have been developed and received much attention in many areas in chemistry study and electrochemical industry [14–16]. Several groups have utilized RTILs as alternative medias for biocatalysis [17,18]. Our group has constructed an excellent electrochemical biosensor based on RTIL ($BPPF_6$), sodium alginate (SA) and graphite for the determination of H_2O_2 [19]. Electrodepositing gold nanoparticles onto the surface of the CPE was another strategy to enhance the sensitivity of the immunosensor. Many works had been conducted to construct the immunosensor using CPE modified with gold nanoparticles [20–26]. However, to the best of our knowledge, none immunosensor based on CPE modified with RTIL and gold nanoparticles has been reported.

As a well-known tumor marker, α-fetoprotein (AFP) is widely used for the diagnosis of patients with germ cell tumors and hepatocellular carcinoma [27–29]. Thus, it is necessary to detect AFP for the clinical diagnosis, especially for early detection of liver carci-

* Corresponding author. Tel.: +86 10 62792343; fax: +86 10 62792343.
E-mail address: jmlin@mail.tsinghua.edu.cn (J.-M. Lin).

0039-9140/$ – see front matter © 2009 Elsevier B.V. All rights reserved.
doi:10.1016/j.talanta.2009.01.036

noma. In recent years, numerous immunological methods for AFP detection have been described [30–33]. Liu and co-workers has proposed a novel reusable electrochemical immunosensor for AFP based on phenylboronic acid monolayer on gold [34]. Yuan and co-workers has constructed some electrochemical immunosensors based on gold nanoparticles, silver nanoparticles and CdS nanoparticles with the detection limits ranging from 0.12 to 2.4 ng mL^{-1} [35–38]. Ye et al. developed novel fluorescent Tb^{3+} chelate-doped silica nanoparticles with surfacing amino groups for time-resolved fluoroimmunoassay of human AFP. The assay response is linear from 0.10 to about 100 ng mL^{-1} with the detection limit of 0.10 ng mL^{-1} [39]. Zhang et al. has developed a new voltammetric enzyme-linked immunoassay system of 3-hydroxyl-2-aminopyridine (HAP)–H_2O_2–horseradish peroxidase (HRP) for the assay of AFP in human serum ranging from 0.1 to 200 ng mL^{-1} with a detection limit of 0.1 ng mL^{-1} [40].

In this study, a novel electrochemical immunosensor based on RTIL ($BPPF_6$), gold nanoparticles and graphite was constructed for the determination of AFP. It was expected that replacing silicone oil with $BPPF_6$ would enhance the current intensity, and the gold nanoparticles on the surface of the electrode could amplify the signal significantly. Moreover, the electrochemical immunosensor could also be renewed easily by mechanical polishing whenever needed.

2. Experimental

2.1. Materials

An AFP ELISA kit, containing a series of AFP standard solutions and polyclonal anti-human-AFP antibody labeled with horseradish peroxidase (HRP-labeled anti-AFP), was purchased from Zhengzhou Bosai Biotechnology (China). Anti-mouse-AFP monoclonal Ab (AFP-McAb) was purchased from Meiao Biotechnology (China). Bovine serum albumin (BSA)-fraction was from AiBi Chemistry Preparation (China). *O*-Aminophenol (OAP) was obtained from Beijing Hengyezhongyuan Limited (China). H_2O_2 (Shanghai Chemical Plant, China) was of analytical grade and used as received. 1-Ethyl-3-(3-dimethylaminopropyl)carbodiimide solution (EDC) and *N*-hydroxysuccinimide solution (NHS) were purchased from Sigma. The ionic liquid *N*-butylpyridinium hexafluorophosphate ($BPPF_6$, 97%, melting point 65 °C) was purchased from Hangzhou Chemer Chemical Limited (China). Graphite powder (average particle size 30 μm) was obtained from Shanghai Colloid Chemical (China) and used without further treatment. The supporting electrolyte solution was 0.1 M phosphate buffered saline (PBS, pH 7.5) containing 0.1 M KCl. All other reagents used were of analytical grade and doubly distilled water was used throughout.

2.2. Apparatus

Cyclic voltammetry (CV) was performed on a CHI 832B electrochemical analyzer (Shanghai ChenHua Instrument, China) with a three-electrode system composed of a platinum wire as auxiliary electrode, an Ag/AgCl/KCl (sat) electrode as reference electrode and the HRP-anti-AFP/CILE as working electrode. Electrochemical impedance spectroscopy (EIS) was carried out on CHI 660C electrochemical analyzer (Shanghai Chenhua Instrument Company, China) with the same three-electrode system described above. All the electrochemical experiments were performed at an ambient temperature of 25 ± 2 °C. Scanning electron microscopy (SEM) measurements were carried out on a JSM-6700F scanning electron microscope (Japan Electro Company). Gold nanoparticles deposition was made on Potentiostat/Galvanostat Model 263A (America).

2.3. Procedure

2.3.1. Construction of CPE and CILE

The ionic liquid carbon paste electrode (CILE) was fabricated with the following procedure: 9 g graphite powder, 3 g ionic liquid $BPPF_6$ (mp 65 °C) and 3 g paraffin were hand-mixed thoroughly in a mortar and heated at a temperature of 80 °C to form a homogeneous carbon paste. A portion of the carbon paste was filled firmly into one end of a glass tube (inner diameter 0.35 cm), and a copper wire was inserted through the opposite end to establish an electrical contact. It was then left to cool to room temperature. Prior to use, a mirror-like surface was obtained by smoothing the electrode on a weighing paper.

2.3.2. Electrodeposition of gold nanoparticles onto CILE

The CILE was immersed into 6 mM $HAuCl_4$ solution containing 0.1 M KNO_3 (prepared in doubly distilled water, and deaerated by bubbling with nitrogen). A constant potential of −0.4 V versus Ag/AgCl was applied for 400 s. Then, the modified electrode (nano-Au–CILE) was washed with doubly distilled water and dried carefully. The electrode was characterized by cyclic voltammetry in 0.1 M HCl and SEM.

2.3.3. Fabrication of the immunosensor

The nano-Au/CILE was electrochemically cleaned by cyclic scanning with a potential range of 0.1–1.5 V in 0.1 M H_2SO_4 at a scan rate of 0.1 V s^{-1}. The nano-Au/CILE was first dipped in 5 mM thioglycolic acid (TGA) aqueous solution for 24 h to form self-assembled monolayer, and then rinsed thoroughly with doubly distilled water to remove extra TGA. The electrode was inverted and activated by being rinsed in 20 μL of solution containing EDC and NHS in 50 mM PBS (pH 7.0), and then evaporated to dryness. After rinsing, the α-fetoprotein immunosensor has developed by covalently conjugating AFP-McAb with TGA on the Nano-Au covered electrode. The unreacted TGA-activated surface groups were subsequently passivated by reaction with 1% (w/w) BSA at room temperature for 2 h.

The AFP immunosensor was based on a sandwich immunoassay method. Before measurement, it was incubated with different concentrations of AFP and excessive HRP labeled AFP antibody in turn at 37 °C for 0.5 h, and the formed immunoconjugation in the immunosensor was detected in an OAP–H_2O_2–HRP electrochemical system. The fabricated AFP immunosensor was stored at 4 °C when not in use. The fabrication process is shown in Scheme 1.

2.3.4. Electrochemical measurements

The electrochemical characterizations and measurements on the modified electrode were carried out using cyclic voltammetry and differential pulse voltammetry (DPV) from −0.6 to 0.1 V (versus Ag/AgCl) in 2 mL of 0.1 M PBS containing 5 mM OAP and 1 mM H_2O_2 at room temperature. The EIS were performed in a solution of 0.01 M PBS (7.4) containing 0.1 M KCl and 5 mM $Fe(CN)_6^{3-}/Fe(CN)_6^{4-}$ with the frequencies ranging from 1 to 10^4 Hz.

3. Results and discussion

3.1. Morphologies of the different electrodes

The response of a biosensor is related to its physical morphology. The SEM of CPE, CILE, nano-Au/CILE and HRP-Ab/AFP/Ab/TGA/nano-Au/CILE were shown in Fig. 1. Significant differences in the surface structure of CPE and CILE are observed. The surface of the CPE was predominated by isolated and irregularly shaped graphite flakes and separated layers were seen (Fig. 1A). The SEM image of CILE showed more uniform surface and no separated carbon layers could

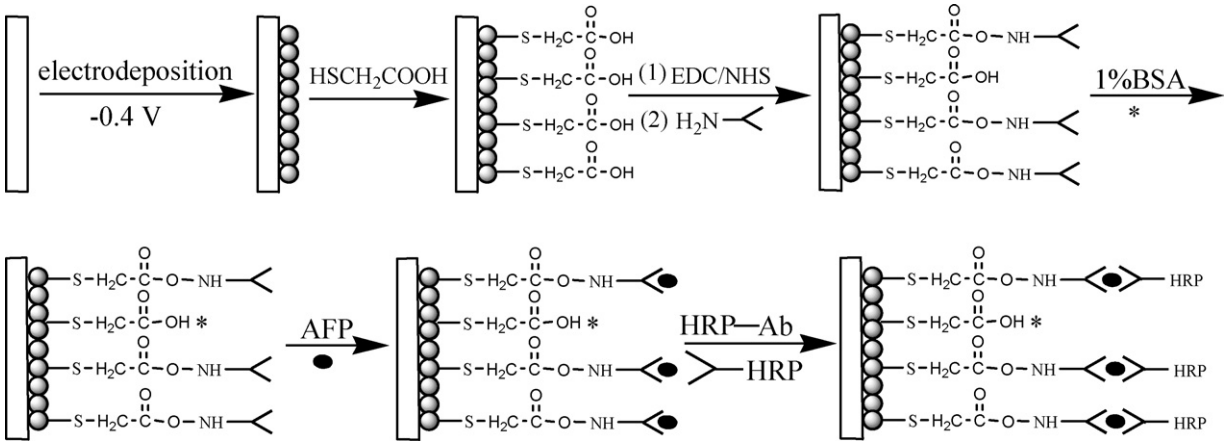

Scheme 1. Schematic illustration of the stepwise immunosensor fabrication process.

be observed in Fig. 1B. It was shown that a mass of RTIL had been embedded in carbon layers [41]. As a liquid with good conductivity and high viscosity, RTIL is capable of better dispersing the graphite powder in the paste than the conditional paraffin, thus could better bridge the graphite flakes. multilayer nanoparticles with an irregular distribution and interstices among the nanoparticles were observed in SEM image of the nano-Au/CILE (Fig. 1C), exhibiting large surface area. Quite different aggregative morphology was shown in Fig. 1D, showing HRP-Ab/AFP/Ab complex had been formed on gold nanoparticles, and the surface area of the electrode increased further.

3.2. Deposition of gold nanoparticles on the CILE

Nano-Au was electrochemically deposited on the surface of CILE at the potential of −0.4 V. The amount of nano-Au deposited can be determined and controlled by the electric quality passing through the cell. The nano-Au film on CILE was electrochemically characterized using CV in 0.1 M HCl at a scan rate of 0.1 V s^{-1}, as shown in Fig. 2b. For comparison, the voltammogram of bare CILE with the same geometric surface area is also presented in Fig. 2a. Nano-Au reduction started at about 1.0 V, showing two reductive current peaks.

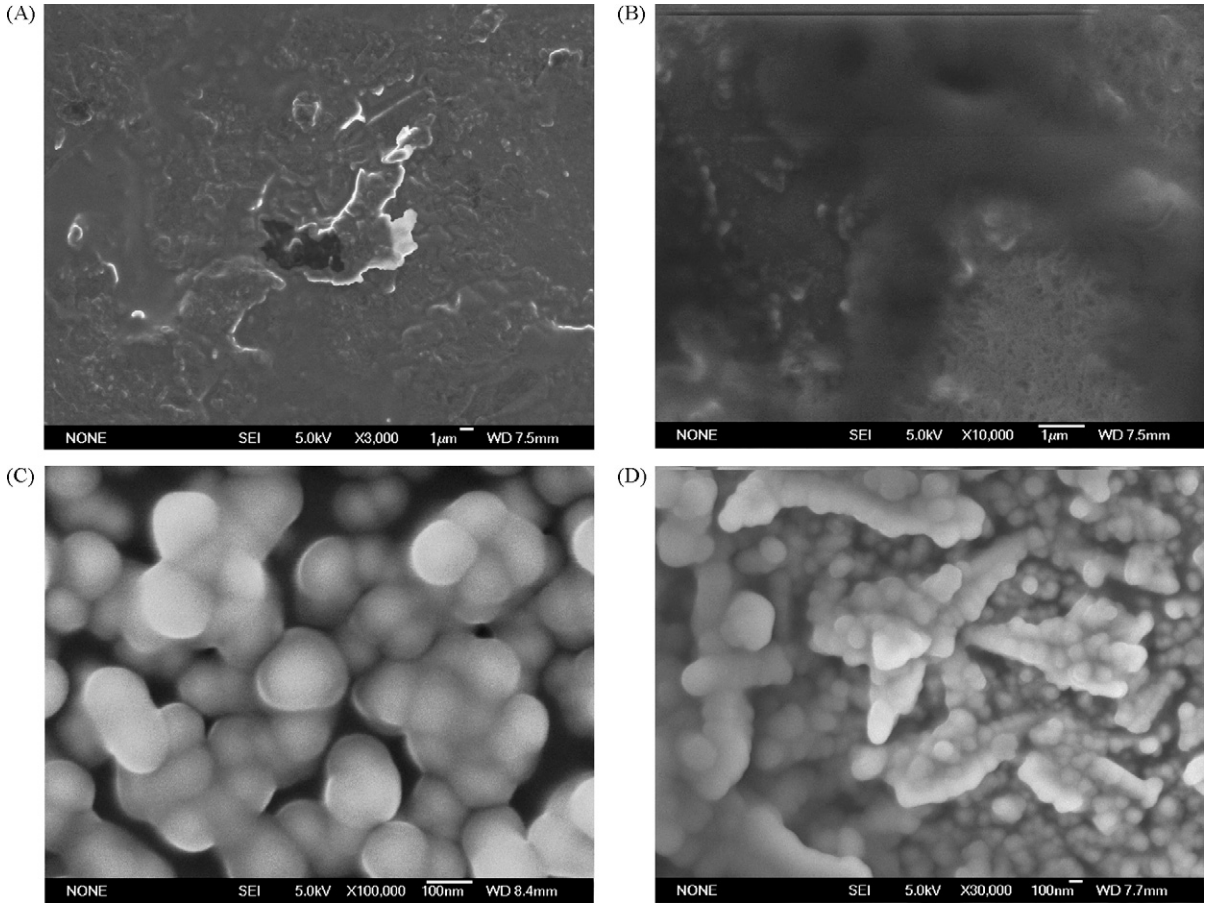

Fig. 1. SEM images of the different types of modified electrodes: (A) CPE; (B) CILE; (C) nano-Au/CILE; (D) HRP-Ab/AFP/Ab/TGA/nano-Au/CILE.

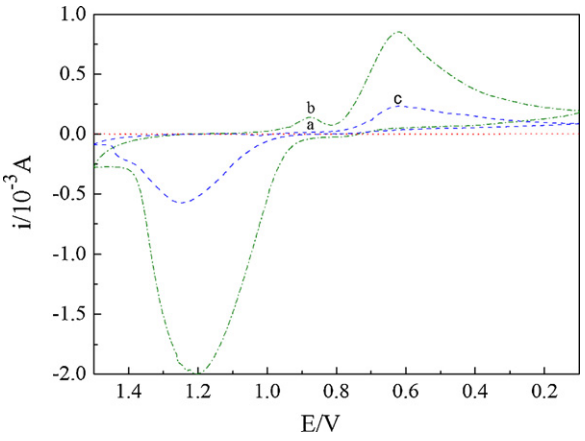

Fig. 2. Cyclic voltammograms (CV) for (a) bare CILE; (b) nano-Au/CILE; (c) nano-Au/CPE in 0.1 M HCl at a scan rate of 0.1 V s^{-1}.

From experimental results and related documents [42], the following electrode mechanism can be proposed:

Oxidation process at 1.21 V

$$Au_{nano} + H^+ + 4Cl^- - 3e^- \rightarrow AuCl_4^- + H^+$$

Reduction processes at 0.64 and 0.88 V

$$AuCl_4^- + e^- \rightarrow AuCl_3^- + Cl^-$$

$$AuCl_3^- + 2e^- \rightarrow Au_{nano} + 3Cl^-$$

For comparison, the CV pattern of nano-Au modified CPE (i.e. without RTIL) was shown in curve c. It can be clearly seen that the peak positions were similar to those in curve b, but the peak currents was about just a quarter of the latter's, showing the conductivity of nano-Au modified CILE was much higher than that of nano-Au modified CPE.

3.3. Electrochemical characteristics of the CILE surface

All electrochemical measurements were performed in 0.01 M PBS solution containing 0.1 M KCl and 5 mM $Fe(CN)_6^{3-/4-}$. The CV of ferricyanide was chosen as a marker to investigate the changes of the electrode behavior before and after each assembly step. Fig. 3A shows the CV of $Fe(CN)_6^{3-/4-}$ at the bare CILE (curve a), nano-Au/CILE (curve b), TGA/nano-Au/CILE (curve c), Ab/TGA/nano-Au/CILE (curve d), AFP/Ab/TGA/nano-Au/CILE (curve e), HRP-Ab/AFP/Ab/TGA/nano-Au/CILE (curve f), respectively. As shown in Fig. 3A, it was observed that the peak current of nano-Au/CILE greatly increased after the modification of nano-Au. Obviously, the nano-Au film increase of conductivity and stability. Moreover, three-dimensionally ordered nano-Au film electrode had a much larger effective surface area than the geometrical surface area, as a result of the efficient alignment of the McAb molecules. Stepwise modifications on the nano-Au/CILE was accompanied by decreases in amperometric response and increases in the peak-to-peak separation between the cathodic and anodic waves of the redox probe, showing that the electron-transfer of $Fe(CN)_6^{3-/4-}$ was obstructed. After the nano-Au film electrode was functionalized with TGA, the electron transfer between the electrochemical probe and electrode surface was inhibited, owing to the electrostatic repulsion between TGA with negative charges and the negatively charged electrochemical probe. When McAb, AFP and HRP-Ab were immobilized on the electrode surface in turn, the peak currents of the redox couple of $Fe(CN)_6^{3-/4-}$ decreased further.

EIS is an effective tool for studying the interface properties of surface-modified electrodes. The typical impedance spectrum (presented in the form of the Nyquist plot) includes a semicircle portion at higher frequencies corresponding to the electron-transfer-limited process and a linear part at lower frequency range representing the diffusion limited process. The semicircle diameter in the impedance spectrum equals the electron-transfer resistance, R_{et}. This resistance controls the electron-transfer kinetics of the redox probe at the electrode interface. Therefore, R_{et} can be used to describe the interface properties of the electrode. Its value varies when different substances that are adsorbed onto the electrode surface [43]. The complex impedance was displayed as the sum of the real and imaginary components (z_{re} and z_{im}). To obtain the detailed information of the impedance spectroscopy, a simple equivalent circuit model was used to fit the results. Fig. 3B showed the impedance spectra observed upon the stepwise modification process. The CILE revealed a very small semicircle domain (curve a), implying a very low electron-transfer resistance of the redox probe. After the CILE was modified with nano-Au, the R_{et} was a smaller semicircle domain near to linear (curve b), showing that the nano-Au/CILE promoted conductivity. When the electrode was conjugated with TGA, the R_{et} slightly increased (curve c). This was attributed to that the self-assembled layer of COO^- terminal groups on the electrode surface generated a negatively charged surface, which reduced the ability of the redox probe to access the layer [44]. Subsequently, after McAb, AFP and HRP-Ab were immobilized on the electrode surface, the R_{et} increased again. The results were consistent with the CV curves shown in Fig. 3A. In comparison with CV, the EIS presented more apparent differences to multilayers deposited on the CILE, indicating better sensitivity.

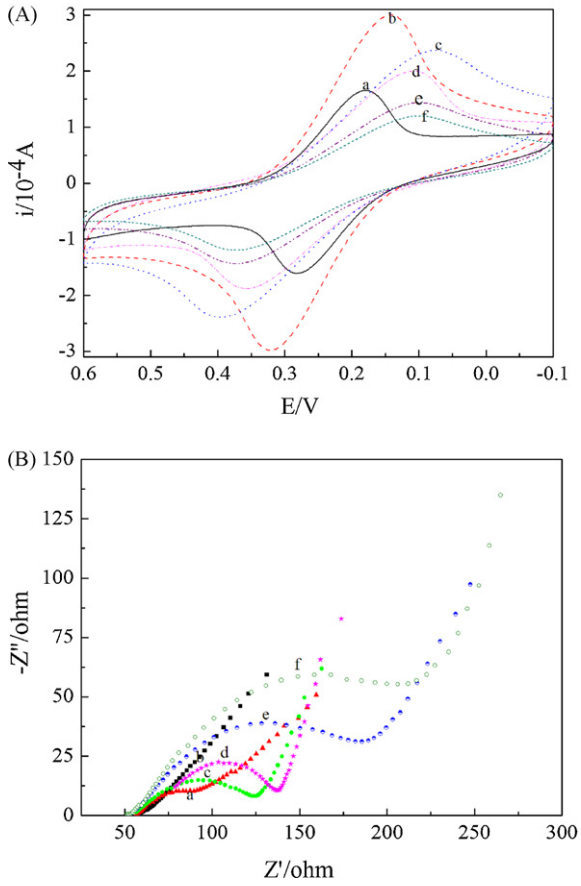

Fig. 3. Cyclic voltammograms (CV) curves (A) and electrochemical impedance spectroscopy (B) of different electrode in PBS (10 mM, pH 7.4) solution containing 0.1 M KCl and 5 mM $Fe(CN)_6^{3-}/Fe(CN)_6^{4-}$; (a) bare CILE; (b) nano-Au/CILE; (c) TGA/nano-Au/CILE; (d) Ab/TGA/nano-Au/CILE; (e) AFP/Ab/TGA/nano-Au/CILE; (f) HRP-Ab/AFP/Ab/TGA/nano-Au/CILE. Scan rate: 0.1 V s^{-1}, quiet time: 2 s.

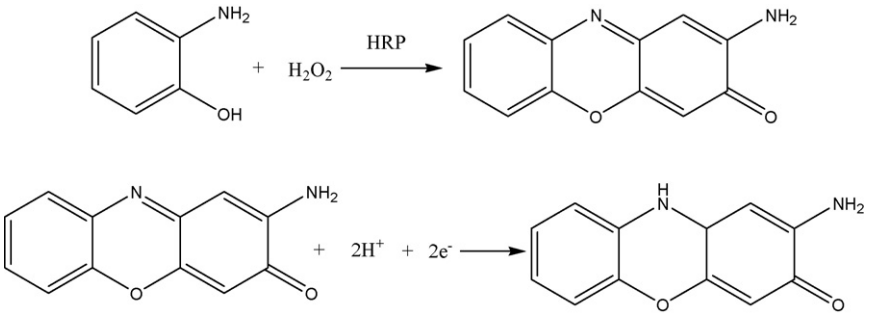

Scheme 2. Response mechanism of HRP to H_2O_2 and OAP.

3.4. CV behavior of the HRP-anti-AFP modified electrodes

It is well known that HRP can catalyze the oxidation reaction of OAP by H_2O_2. The mechanism of enzymatic catalysis and oxidation has been described previously [45]. A possible mechanism of reaction of H_2O_2 catalyzed by HRP is proposed in Scheme 2. Fig. 4 showed the CV of various electrodes in different solutions. No response of the CILE was observed in the absence of OAP and H_2O_2 in 0.1 M pH 7.5 PBS (curve a). Whereas, the CV of CILE showed a pair of obvious redox peaks at −0.25 and −0.34 V (curve b). As three-dimensionally ordered nano-Au/CILE had not only good conductivity and stability, but also a much larger effective surface area, the peak currents of the redox couple became bigger than the bare CILE. But the peak-to-peak separation between the cathodic and anodic waves increased slightly. As to the HRP-Ab/AFP/Ab/TGA/nano-Au/CILE, the redox current attributed to the catalytic process of HRP at the immunosensor increased (curve c). The increased current response indicated the direct electron-transfer of HRP with the aid of nano-Au.

3.5. Influence of the scan rate

Typical CV curves of the HRP-Ab/AFP/Ab/TGA/nano-Au/CILE in 0.1 M PBS (pH 7.5) containing 5.0 mM OAP and 1 mM H_2O_2 at different scan rates were shown in Fig. 5. It can be seen that a pair of roughly symmetric anodic and cathodic peaks appeared with almost equal peak currents in the scan rate range from 0.03 to 0.45 V s^{-1}. The peak-to-peak separation also increased with the scan rate. A good linear relationship was found for the peak current and scan rate, with the results shown in Fig. 5 (upper left inset). The reduction and oxidation peak currents rise linearly with the linear regression equations as i_{pc} (10^{-4} A) = $7.4276\nu^{1/2}$ (V s^{-1})$^{1/2}$ − 0.2494 (n = 10, γ = 0.9987), i_{pa} (10^{-4} A) = $-10.077\nu^{1/2}$ (V s^{-1})$^{1/2}$ − 0.6483 (n = 10, γ = 0.9994), respectively, suggesting that the reaction is a quasi-reversible diffusion-controlled behavior with an electron transfer process.

3.6. Optimization of experimental conditions

The experimental conditions, which can affect the amperometric determination of AFP, including the time of electrodeposition, the pH of supporting electrolyte, the incubation temperature and time of immunoreaction were optimized.

The peak current increased with the deposition time. When the deposition time reached 400 s, at the potential of −0.4 V (versus Ag/AgCl) in 6 mM $HAuCl_4$, the nano-Au/CILE surface was found to be best and the current response in 0.1 M HCl increased slightly. So the electrodeposition time optimum was 400 s (Fig. 6A).

The acidity of the solution greatly affects the enzyme activity. So the pH value of substrate solution was the important factor to the current response. The influence of the pH of the assay solution in 0.1 M PBS containing 5 mM OAP and 1 mM H_2O_2 was investigated. The pH optimum was 7.5. Thus, pH 7.5 (Fig. 6B) was fixed for the rest of the experiments.

The influences of the antigen–antibody incubation temperature and time on the amperometric responses were also studied. The optimum conditions were 37 °C and 0.5 h (Fig. 6C and D).

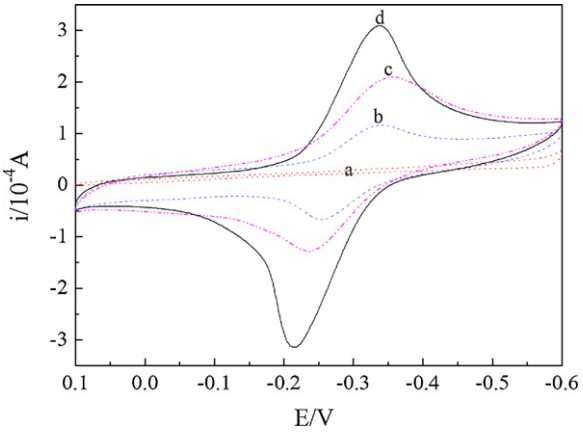

Fig. 4. Cyclic voltammograms (CV) of different electrodes: (a) bare CILE in PBS (0.1 M, pH 7.5); (b) bare CILE in PBS (0.1 M, pH 7.5) containing 5 mM OAP and 1 mM H_2O_2; (c) nano-Au/CILE in PBS (0.1 M, pH 7.5) containing 5 mM OAP and 1 mM H_2O_2; (d) HRP-Ab/AFP/Ab/TGA/nano-Au/CILE in PBS (0.1 M, pH 7.5) containing 5 mM OAP and 1 mM H_2O_2. Scan rate: 0.10 V s^{-1}, quiet time: 2 s.

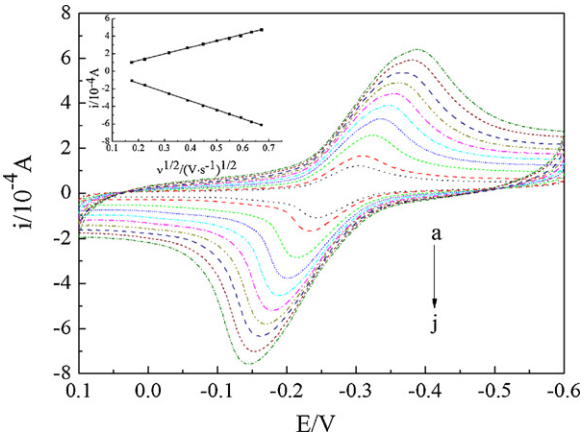

Fig. 5. Cyclic voltammograms (CV) of HRP-Ab/AFP/Ab/TGA/nano-Au/CILE in 0.1 M PBS (pH 7.5) containing 5.0 mM OAP and 1 mM H_2O_2 at: (a) 0.03; (b) 0.05; (c) 0.10; (d) 0.15; (e) 0.20; (f) 0.25; (g) 0.30; (h) 0.35; (i) 0.40; (j) 0.45 V s^{-1}. The inset show a calibration plot of peak current versus scan rate.

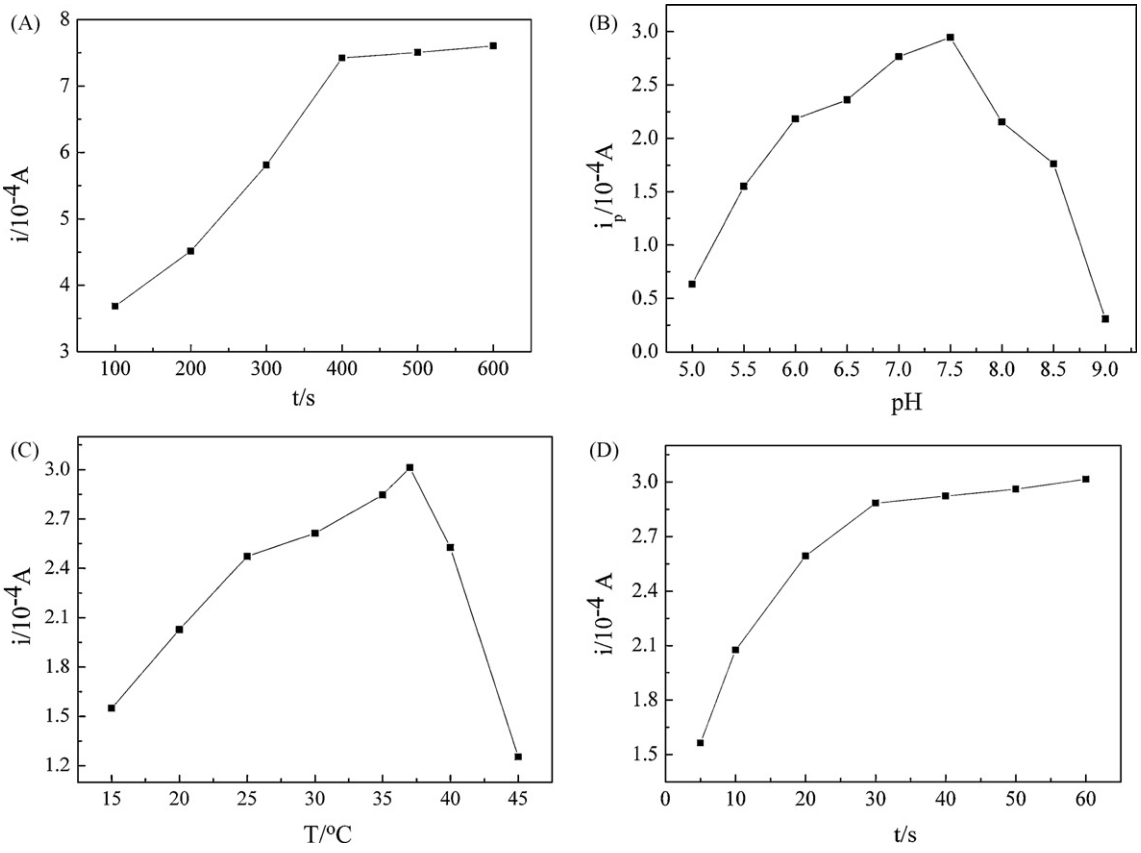

Fig. 6. Optimization of experimental conditions. (A) The time of electrodeposition; (B) the pH of supporting electrolyte; (C) the incubation temperature; (D) time.

3.7. Analytical performance

Under the optimized experimental conditions mentioned above, the relationship between the peak current and the concentration of AFP was investigated. As presented in Fig. 7, the amperometric response increased with the increase of AFP concentration from 0.5 to 80 ng mL^{-1} with a correlation coefficient of 0.9948. The regression equation was Δi (10^{-4} A) = 0.1655C (ng mL^{-1}) + 2.1453, where i is the current intensity, and C is the AFP concentration. The detection limit (3σ, n = 11) is estimated to be 0.25 ng mL^{-1}. A series of 11 repetitive measurements of 1.0 ng mL^{-1} AFP are used for estimating the precision and the relative standard deviation (R.S.D.) is 2.3%, indicating an acceptable level of the precision for the immunoassay.

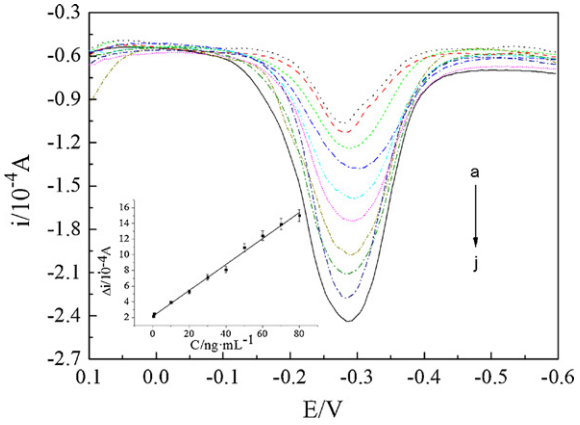

Fig. 7. The differential pulse voltammograms (DPV) of different AFP concentration obtained at HRP-Ab/AFP/Ab/TGA/nano-Au/CILE in PBS (0.1 M, pH 7.5) containing 5 mM OAP and 1 mM H_2O_2; (a) 0.5; (b) 1; (c) 10; (d) 20; (e) 30; (f) 40; (g) 50; (h) 60; (i) 70; (j) 80 ng mL^{-1}. The inset show a calibration plot of peak current versus OAP concentration.

3.8. Selectivity and stability of immunosensor

Selectivity is also important in practical use of the biosensors. The specific analyte has to be measured in the presence of a relatively high amount of nonspecific species in diagnostic applications. In this study, four kinds of potentially interferent, including L-glutamic acid, BSA, hemoglobin and D-glucose were used to evaluate the selectivity of the immunosensor. 50 ng mL^{-1} AFP was detected with the established sensor in the presence of these interferents of various concentrations ranging from 1 to 10 μg mL^{-1} under the optimized situation. The responses, shown as the relative value to that generated by mere 50 ng mL^{-1} AFP, was shown in Table 1. It can be seen that the interferents of relatively high concentrations only posed negligible affection on AFP detection, showing the established sensor had high selectivity.

The storage stability of the sensor was studied by storing it at 4 °C when not in use and measured intermittently. Five days later the response of the sensor still retained 96% and after two weeks the response still retained 90% of the initial. The good stability could be

Table 1
The relative responses of 50 ng mL^{-1} AFP in the presence of interferent on the established sensor (compared to the response mere 50 ng mL^{-1} AFP)*.

Interferents	Concentrations (μg mL^{-1})	Relative responses
L-Glutamic acid	1	0.9974
BSA	10	0.9743
Hemoglobin	140	1.003
D-Glucose	1	0.9865

* Each value is the average of three measurements.

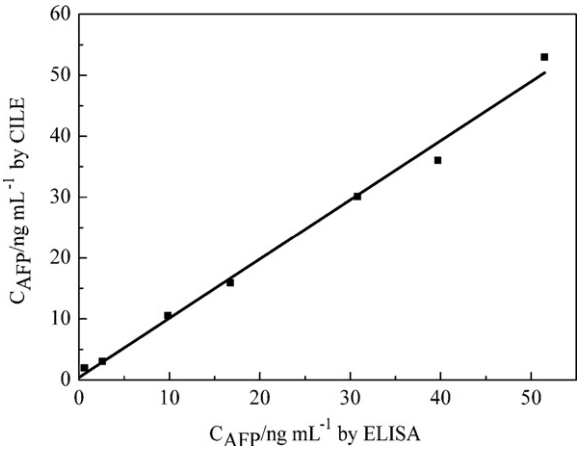

Fig. 8. Correlation of proposed electrochemical immunoassay for human serum samples against ELISA.

Table 2
AFP concentration in clinical sera.

Sample	Proposed method (ng mL^{-1})	ELISA (ng mL^{-1})	Relative deviation (%)
1	283.4	264.3	7.2
2	13.76	14.91	−7.7
3	162.5	151.6	6.7

Higher serum AFP levels could be detected with an appropriate dilution.

due to the good biocompatibility of the nano-Au film aqueous solution. Moreover, the nanostructure of Au greatly enhances the active surface available for protein molecules binding over the geometrical area.

3.9. The corelationship of electrochemical immunosensor and ELISA for detection of AFP in clinical serum samples

Some clinical sera were analyzed using the electrochemical immunosensor as well as the reference ELISA. The calibration curve between proposed method and ELISA was shown in Fig. 8. The regression equation could be expressed as $Y = 0.9722X + 0.3685$ (X was the concentration of AFP detected by the proposed method, ng mL^{-1}, Y was the concentration of AFP detected by ELISA method, ng mL^{-1}, $n = 7$, $\gamma = 0.9933$). In order to assess the accuracy and applicability of the present method, three serum samples were determined and the results were compared with the standard ELISA method (Table 2). It can be seen obviously that this developed electrochemical immunoassay may provide an alternative method for liver cancer biomarkers diagnosis in clinical analysis.

4. Conclusion

In the present work, novel immunosensor based on CPE constructed of RTIL and gold nanoparticles was used for electrochemical determination of human AFP. The combination of the good conductivity of RTIL and the advantages of the gold nanoparticles, including biocompatibility and amplification, enhanced the sensitivity of the immunosensor significantly. The results showed that the method was simple and sensitive enough for determination of AFP in human serum samples with good precision and accuracy. It can be expected that the new immunoassay would be widely useful for highly sensitive clinical analysis and other biotechnology applications.

Acknowledgments

This work was supported by the Excellent Young Scientists Encouragement Foundation of Shandong Province (No. 2008BS05004), the Educational Administration of Shandong Province (No. J07YC09) and the National Natural Science Foundation of China (No.20775038).

References

[1] T.C. Tang, A. Deng, H.J. Huang, Anal. Chem. 74 (2002) 2617.
[2] K. Sato, A. Hibara, M. Tokeshi, H. Hisamoto, T. Kitamori, Adv. Drug. Deliv. Rev. 55 (2003) 379.
[3] M.S. Wilson, Anal. Chem. 77 (2005) 496.
[4] T. Konry, A. Novoa, Y. Shemer-Avni, N. Hanuka, Anal. Chem. 77 (2005) 1771.
[5] B.L. Zuo, S.M. Li, Z. Guo, J.F. Zhang, C.Z. Chen, Anal. Chem. 76 (2004) 3536.
[6] R. Kurita, Y. Yokota, Y. Sato, F. Mizutani, O. Niwa, Anal. Chem. 78 (2006) 5525.
[7] B.Y. Won, H.G. Choi, K.H. Kim, S.Y. Byun, Biotechnol. Bioeng. 89 (2005) 815.
[8] J. Wang, L. Fang, J. Am. Chem. Soc. 120 (1998) 1049.
[9] J. Kulys, Biosens. Bioelectron. 14 (1999) 473.
[10] C.M.V.B. Almeida, B.F. Giannetti, Electrochem. Commun. 4 (2002) 985.
[11] D. Moscone, D.D. Ottavi, D. Compagnone, G. Palleschi, A. Amine, Anal. Chem. 73 (2001) 2529.
[12] N.S. Lawrence, R.P. Deo, J. Wang, Anal. Chem. 76 (2004) 3735.
[13] P. Tomcik, C.E. Banks, T.J. Davies, R.G. Compton, Anal. Chem. 76 (2004) 161.
[14] T. Welton, Chem. Rev. 99 (1999) 2071.
[15] F. Endres, ChemPhysChem 3 (2002) 144.
[16] M.C. Buzzeo, R.G. Evans, R.G. Compton, ChemPhysChem 5 (2004) 1106.
[17] S. Park, R. Kazlauskas, Curr. Opin. Biotechnol. 14 (2003) 432.
[18] J.A. Laszlo, D.L. Compton, J. Mol. Catal. B: Enzym. 18 (2002) 109.
[19] C.F. Ding, M.L. Zhang, F. Zhao, S.S. Zhang, Anal. Biochem. 378 (2008) 32.
[20] H.X. Ju, S. Liu, B. Ge, F. Lisdat, F.W. Scheller, Electroanalysis 14 (2002) 141.
[21] M.B. González-García, C. Fernández-Sánchez, A. Costa-García, Biosens. Bioelectron. 15 (2000) 315.
[22] M.L. Mena, P. Yáñez-Sedeño, J.M. Pingarrón, Anal. Biochem. 336 (2005) 20.
[23] J. Manso, L. Agüí, P. Yáñez-Sedeño, J.M. Pingarrón, Anal. Lett. 37 (2004) 887.
[24] L. Agüí, J. Manso, P. Yáñez-Sedeño, J.M. Pingarrón, Sens. Actuators B 113 (2006) 272.
[25] L. Agüí, J. Manso, P. Yáñez-Sedeño, J.M. Pingarrón, Talanta 64 (2004) 1041.
[26] L. Agüí, C. Peña-Farfal, P. Yáñez-Sedeño, J.M. Pingarrón, Talanta 74 (2007) 412.
[27] E. Alpert, R. Hershberg, P.H. Schur, K.J. Lsselbacher, Gastroenterology 61 (1971) 137.
[28] K. Okuda, Dig. Dis. Sci. 31 (1986) 133.
[29] X.W. Wang, H. Xie, Life Sci. 64 (1999) 17.
[30] M. Xue, T. Haruyama, E. Kobatake, M. Aizawa, Sens. Actuatators B 35 (1996) 458.
[31] Y. Yamagata, H. Katoh, K. Nakamura, T. Tanaka, S. Satomura, S. Matsuura, J. Immunol. Methods 212 (1998) 161.
[32] K. Ito, M. Oda, A. Tsuji, M. Maeda, J. Pharm. Biomed. Anal. 20 (1999) 169.
[33] R. Wang, X. Lu, W. Ma, J. Chromatogr. B 779 (2002) 157.
[34] Z. Wang, Y.F. Tu, S.Q. Liu, Talanta 77 (2008) 815.
[35] Z. Qiang, R. Yuan, Y.Q. Chai, N. Wang, Electrochim. Acta 51 (2006) 3763.
[36] Y. Zhuo, R. Yuan, Y.Q. Chai, D.P. Tang, Electrochem. Commun. 7 (2005) 355.
[37] Y. Zhuo, R. Yuan, Y.Q. Chai, Y. Zhang, Sens. Actuators B 114 (2006) 631.
[38] X.M. Miao, R. Yuan, Y.Q. Chai, Y.T. Shi, Biochem. Eng. J. 38 (2008) 9.
[39] Z.Q. Ye, M.Q. Tan, G.L. Wang, J.L. Yuan, Talanta 65 (2005) 206.
[40] S.S. Zhang, J. Zou, F.L. Yu, Talanta 76 (2008) 122.
[41] T.E. Sutto, P.C. Trulove, H.C. DeLong, Electrochem. solid-State Lett. 6 (2003) 50.
[42] M.B.G. García, A.C. García, Bioelectrochem. Bioenerg. 38 (1995) 389.
[43] Y.J. Liu, F. Yin, Y.M. Long, Z.H. Zhang, S.Z. Yao, Colloid Interface Sci. 258 (2003) 75.
[44] Z.P. Li, C.H. Liu, Y.Q. Su, X.R. Duan, Chem. J. Internet 7 (2005) 83.
[45] Y.N. He, H.Y. Chen, J.J. Zheng, G.Y. Zhang, Z.L. Chen, Talanta 44 (1997) 823.